



Shear and extensional rheology of hydroxypropyl cellulose melt using capillary rheometry

Anant Paradkar^{a,c}, Adrian Kelly^b, Phil Coates^b, Peter York^{c,*}

^a Department of Pharmaceutics, Bharati Vidyapeeth University, Poona College of Pharmacy, Pune, India

^b IRC in Polymer Engineering, University of Bradford, Bradford BD7 1DP, UK

^c Institute of Pharmaceutical Innovation, University of Bradford, Bradford BD7 1DP, UK

ARTICLE INFO

Article history:

Received 4 July 2008

Received in revised form

30 September 2008

Accepted 17 November 2008

Available online 25 November 2008

Keywords:

Hydroxypropyl cellulose

Polymer melt rheology

Capillary rheometry

Hot melt extrusion

ABSTRACT

With increasing interest in hot melt extrusion for preparing polymer–drug systems, knowledge of the shear and extensional rheology of polymers is required for the formulation and process design. Shear and extensional rheology of three commercial grades of hydroxypropyl cellulose (HPC) was examined at 140, 145 and 150 °C using twin bore capillary rheometry at range of processing rates. The power law model fitted for shear flow behaviour up to shear strain rates of approximately 1000 s⁻¹, above which measured shear viscosities deviated from the power law and surface instabilities were observed in the extrudate, particularly for higher molecular weight grades. Shear thinning index was found to be relatively independent of temperature and molecular weight, whilst the consistency index, indicative of zero shear viscosity increased exponentially with increase in molecular weight. Extensional viscosity of all grades studied was found to decrease with increasing temperature and increasing processing rate. Foaming of the extrudate occurred especially at low temperatures and with the high molecular weight grade. An understanding of the relationships between shear and extensional flows with temperature, processing rate and molecular weight is a useful tool for process design; optimisation and troubleshooting of Hot melt extrusion (HME) of pharmaceutical formulations.

© 2008 Elsevier B.V. All rights reserved.

1. Introduction

HME technology has been widely used in the plastic and rubber industry. During HME, the molten plastic mass containing polymer and other suitable additives such as plasticizers and thickening agents are melted by the action of an Archimedian screw rotating in a heated barrel and forced at high temperature through a die. This contrasts with the injection moulding process in which molten polymer is injected into a mould cavity at high pressure to form a complex shape. HME is a solvent-free and continuous processing technique currently being explored for its applications for pharmaceuticals. The applicability of HME has been demonstrated for the development of solid dispersions [1–3], transdermal and bioadhesive films [4,5], suppositories [6], pellets [7] and tablets [8,9].

Commonly used polymers for HME include polyvinylpyrrolidone and its co-polymers, polyethylene oxide, cellulose ethers, acrylic acid derivatives and biodegradable aliphatic polyesters like polylactide, polyglycolide and their co-polymers.

* Corresponding author at: Institute of Pharmaceutical Innovation, University of Bradford, Bradford, UK BD7 1DP. Tel.: +44 1274 233900; fax: +44 1274 236155.

E-mail address: P.York@bradford.ac.uk (P. York).

These polymers are used in pharmaceutical formulations processed by other technologies and their properties, as related to these technologies, have been studied extensively. In the melt extrusion process, rheology of the polymer melt is an important factor affecting processing conditions and properties of pharmaceutical product. Knowledge of the rheology is required for process optimisation, troubleshooting, design of process equipment and for computational fluid dynamics simulations.

Extruder torque and die head pressure has been studied as indicators of melt viscosity [10,11]. Chokshi et al. [12] studied shear rheology of drug–polymer melt blends and correlated it with polymer–drug miscibility and extrudability. Lyons et al. [13] studied the effect of supercritical fluids on polymer plasticization, extrusion speeds, and temperature of polymer blend using parallel plate rheometry.

Rotational shear rheology has been useful in establishing relationships between material structure and its properties; however these are generally limited to flows in the linear viscoelastic region, which is characterised by small strain and low rate of material deformation. The flow of polymer melt experienced in HME is rapid and largely nonlinear viscoelastic by nature. Extensional properties become important during flow into the die cavity, where melt flow converges and the polymer molecules undergo stretching, alignment and alteration in chain entanglement. Resistance to flow in

convergent regions such as the die entry region are indicated by extensional viscosity and therefore have relevance to HME processing.

1.1. Theory

Capillary rheometry is a pressure-driven technique which mimics flow through an extruder die or injection moulding nozzle, capable of providing shear and extensional rheological properties of the melt at rates experienced during processing. In the range of shear strain rates encountered in conventional polymer processing (10–100,000 s⁻¹) shear flow can be described by the power law Eq. (1).

$$\eta = K \cdot \dot{\gamma}^{(n-1)} \quad (1)$$

where η , $\dot{\gamma}$, K and n denote shear viscosity (Pa s), shear rate (s⁻¹), consistency index and power law index, respectively.

During flow of polymer through the die, the apparent shear rate and shear stress at the wall of a cylindrical die can be derived from the Poiseuille relationship [14]:

$$\dot{\gamma}_{\text{app}} = \frac{4Q}{\pi R^3} \quad (2)$$

$$\tau_{\text{W,app}} = \frac{R\Delta P}{2L} \quad (3)$$

where $\dot{\gamma}_{\text{app}}$ and $\tau_{\text{W,app}}$ denote apparent wall shear rate (s⁻¹) and shear stress (Pa), respectively for the flow of fluid through a capillary having radius R (m) and length L (m), at volumetric flow rate Q (m³/s) across pressure drop ΔP (Pa). Apparent shear viscosity is the ratio of apparent shear stress to shear rate:

$$\eta_{\text{app}} = \frac{\tau_{\text{W,app}}}{\dot{\gamma}_{\text{app}}} \quad (4)$$

Newtonian fluids in laminar flow exhibit a parabolic velocity profile, whilst for polymer melts the flow profile tends to be plug-like. The relationship between $\dot{\gamma}_{\text{app}}$ and $\dot{\gamma}_{\text{true}}$ as shown in Eq. (5) has been derived considering a balance of forces for flow through the capillary.

$$\dot{\gamma}_{\text{true}} = \left(\frac{3n+1}{4n} \right) \cdot \dot{\gamma}_{\text{app}} \quad (5)$$

In order to measure accurately the wall shear stress, the pressure drop across the die should be corrected for the energy required to converge the melt into the entrance of the capillary by measuring the entrance pressure drop. True or Bagley corrected, shear stress (τ) is calculated as

$$\tau_{\text{W}} = \frac{(\Delta P_{\text{L}} - \Delta P_{\text{O}}) \cdot R}{2L} \quad (6)$$

where ΔP_{O} and ΔP_{L} denote pressure drop into the die entrance and across die length, respectively. ΔP_{O} is an indicator of flow convergence and in turn an extensional property of the melt. Extensional viscosity is a measure of a material's resistance to tensile or stretching flow and a number of direct and indirect measurements have been proposed [15–17]. Cogswell treated the analysis of convergent flow by separating the convergent flow into shear and extensional components [15]. This has been modified to treat free convergence (entry semi-angle 90°), which is probably the simplest and most widely used extensional viscosity model.

$$\eta_{\text{E}} = \frac{9}{32} \frac{(n+1)^2}{\eta} \left(\frac{P_{\text{O}}}{\dot{\gamma}} \right)^2 \quad (7)$$

$$\sigma_{\text{E}} = \frac{3}{8} (n+1) P_{\text{O}} \quad (8)$$

$$\dot{\epsilon} = \frac{\sigma_{\text{E}}}{\eta_{\text{E}}} \quad (9)$$

where η_{E} , σ_{E} , and $\dot{\epsilon}$ are extensional viscosity (Pa s), extensional stress (Pa), and extensional strain rate (s⁻¹), respectively. The above derivations are based on the assumptions that flow is isothermal, incompressible and a velocity at the die wall is zero. Errors caused by heat generation and pressure effect on viscosity [18] are assumed to be mutually cancelling [19].

The temperature dependence of shear viscosity is an important parameter in process design and simulation, and a number of models have been used. The simplest of these is an exponential dependence:

$$f(T) = e^{-b(T-Tr)} \quad (10)$$

where T and Tr are temperature and reference temperature, respectively and b is the temperature sensitivity (°C⁻¹). This model is accurate over a small temperature range, whereas the Arrhenius [20] and Williams, Landel and Ferry (WLF) models are also used to describe temperature sensitivity over a wider temperature range [21].

1.2. Capillary rheometry

Capillary rheometers are used to determine shear and extensional properties of the fluid under different shear rates and temperatures which usually occur during HME. The pressure drop at the die entry region which is required for the calculation of extensional viscosity and corrected shear viscosity may be obtained by two methods viz. Bagley method and Cogswell method. In the Bagley method, pressure drop across dies with different length/diameter (L/D) ratio are determined and then pressure drop is extrapolated to calculate pressure drop across zero length die. Extrapolation errors and nonlinearity of data are limitations of this method. In Cogswell's method, a die of the same diameter as the long die but effectively zero length (L/D ratio <0.25) is used for direct measurement of entrance pressure drop. Twin bore capillary rheometers allow two geometries of die to be examined simultaneously, thus corrected shear viscosity and extensional viscosity can be measured during a single test. In addition to measuring viscosity, capillary rheometry can, through the use of specialist test equipment, provide information relating to time dependent behaviour, die swell (a measure of elasticity), melt fibre strength, wall slip velocity and P - V - T data.

This research paper reports shear and extensional viscosity data of different grades of hydroxypropyl cellulose, a commonly used polymer in HME at different temperatures.

2. Materials and methods

2.1. Materials

HPC grades HPC-SSL, HPC-SL and HPC-L (Nisso Chemical Europe GmbH, Germany) were used, with weight average molecular weights of 65,000, 131,000 and 171,000, respectively. These all grades were supplied in powder form.

2.2. Rheometry

The shear and extensional rheology of the three grades of HPC was studied using twin bore (RH10) precision advanced capillary rheometer (Malvern Instruments, UK) using Flowmaster version 8.3.10 control software. A schematic representation of the instrument is shown in Fig. 1. A common crosshead is used to drive twin pistons at a range of speeds causing melt to flow at known flow rate through capillary dies. Pressure drop at the entrance of each capillary die was monitored by the control software. The inner diameter and length of the barrel used were 15 and 240 mm, respectively.

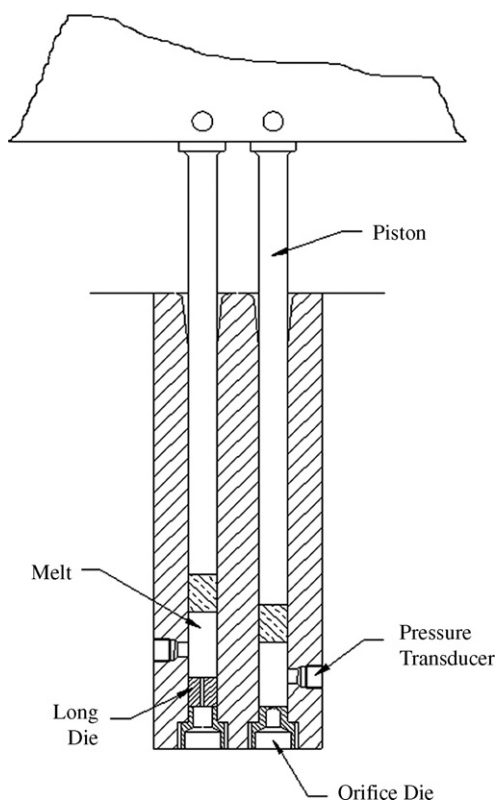


Fig. 1. Schematic representation of a twin bore capillary rheometer.

One barrel of the rheometer was fitted with a capillary die of L/D ratio 16 and the other bore was fitted with an orifice die. The bore diameter of both capillary dies was 1 mm, with die entry angle of 180° , whilst the lengths were 16 and less than 0.25 mm for long and orifice dies, respectively. Capillary dies were fitted into the bottom of the barrels and pressure transducers located directly above the dies. The capillary dies were made from tungsten carbide–cobalt alloy in order to maintain tight geometrical integrity.

The polymer was dried in an oven at 50°C for 24 h before rheological investigation. The flow behaviour of each grade of HPC was characterised at 140, 145 and 150°C . The rheometer was set at test temperature and allowed to stabilize. Temperatures were controlled within $\pm 0.5^\circ\text{C}$ of the set values and monitored by platinum resistance thermometers fitted in the three (top, middle and bottom) zones of the barrel. The polymer was fed into both bores of the barrel and manually compressed before the test was started. The polymer was subjected to pre-compression pressure of 0.5 MPa, and a total pre-heating time of 240 s. The instrument was run in 8-stage discrete speed programme. The piston speed was automatically converted to shear rate by software and is summarised in Table 1.

Table 1
Range of set crosshead speeds and equivalent wall strain rates during capillary rheometry tests.

Test stage number	Piston speed (mm/s)	Apparent wall shear rate (s^{-1})
1	0.03	50.00
2	0.05	96.53
3	0.10	184.75
4	0.20	358.79
5	0.39	694.83
6	0.75	1340.86
7	1.44	2589.69
8	2.78	5000.26

3. Results and discussion

Raw data obtained during the operation of the capillary rheometer was in the form of pressure drop across the long die and the orifice die, at a given flow rate. The values of apparent shear rate, shear stress and apparent shear viscosity were calculated by the control software as per Eqs. (2)–(4), respectively. A characteristic relationship between pressure drop with time for HPC-L, HPC-SL and HPC-SSL grades at 140°C is shown in Fig. 2. At the given temperature both long and orifice die pressure drops increased with piston speed and therefore capillary wall shear rate. The time required to attain equilibrium at first stage increased with viscosity of the melt. Long die pressure drop equilibration at stages up to 1000 s^{-1} was smooth, indicating that steady flow conditions were readily achieved. At higher shear rate stages, especially for high molecular weight grades, measured pressure values showed some fluctuation or localised drops in pressure. Noise in the measured pressure signal can indicate instabilities in the flow prior to, during or upon exit of the capillary die, or the presence of particulate contaminants or unmolten polymer.

The logarithmic relationship between apparent shear viscosity and wall shear rate for the three grades of HPC at different temperatures is shown in Fig. 3. All grades exhibited decreasing viscosity with increasing shear strain rate, otherwise known as shear thin-

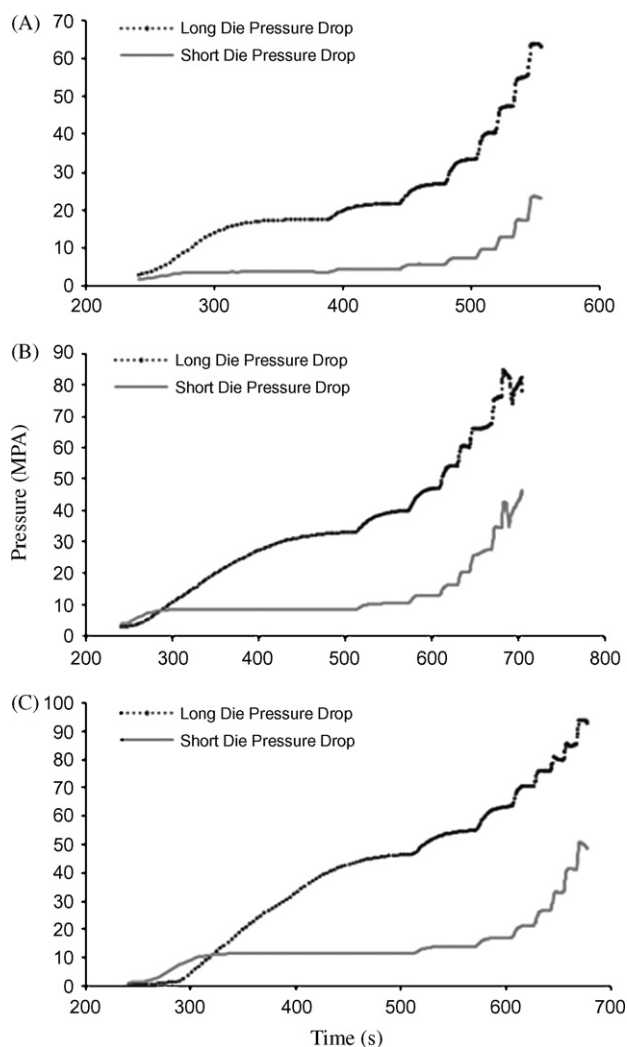


Fig. 2. Measured pressure data from capillary rheometry flow characterisations (A) HPC-SSL; (B) HPC-SL and (C) HPC-L.

Table 2
Calculated power law parameters and temperature sensitivity at each measured test condition.

Grade	M_w	n	K (Pa s ^{<i>n</i>})	Temperature (°C)	Temperature sensitivity (°C ⁻¹)
SSL	65,000	0.24	65,042	140	0.0631
		0.27	44,658	145	
		0.31	31,623	150	
SL	131,000	0.24	164,285	140	0.0736
		0.24	75,145	145	
		0.24	61,589	150	
L	171,000	0.21	237,375	140	0.0767
		0.24	143,747	145	
		0.25	90,908	150	

ning behaviour. This characteristic is common to most widely used commodity polymers and is the main reason why polymers flow readily at high processing rates in the melt phase. It can also be seen that log–log plots of shear viscosity followed a linear relationship with wall shear strain, allowing a simple power law model to be used to describe flow behaviour in this shear rate region. This is an extremely useful flow model as it allows the flow to be characterised by two constants, n and K . Power law index, n , describes the shear thinning nature of the melt and is calculated from the gradient of the shear viscosity versus shear rate plot. K is the consistency index of the melt and is calculated from the intercept of the shear viscosity at zero wall shear rate. In practice, the shear flow behaviour of all polymers is more complex than this simple model suggests, viscosity being constant in the ‘Newtonian’ region at very low shear rates (less than approximately 1 s⁻¹) and also deviating from the power law at very high shear rates (above 10⁶ s⁻¹) but the power law model is adequate for calculations relevant to most pro-

cessing applications. Calculated values of n and K from power law fits of the measured data are summarised in Table 2.

Values of n at all conditions were calculated to be in the range between 0.21 and 0.31, and for grades HPC-SSL and HPC-L appeared to increase with increasing melt temperature. It can be seen that plots of viscosity versus shear rate at three temperatures were parallel at the lower range of shear rates but appeared to converge

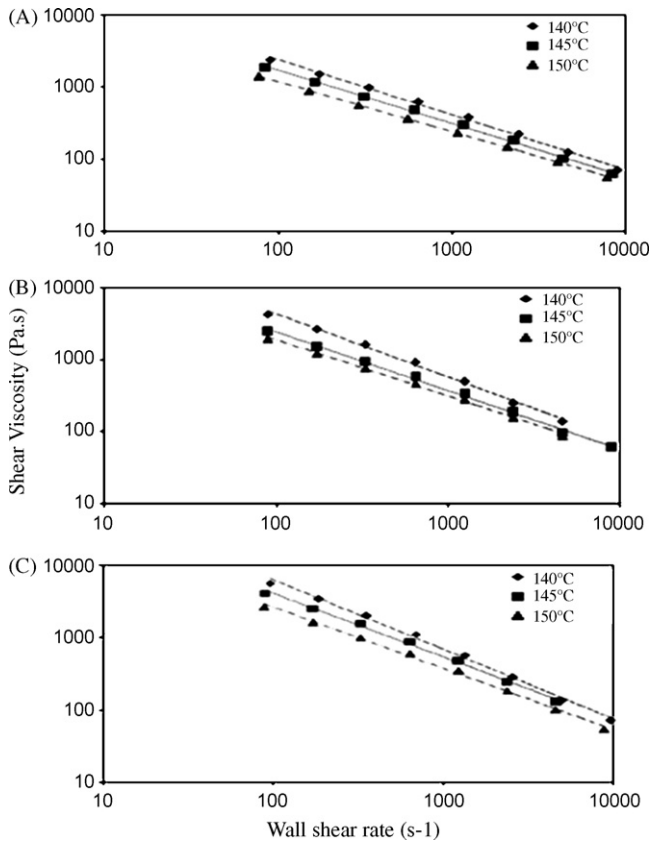


Fig. 3. Temperature dependence of shear viscosity with power law curve fit (A) HPC-SSL; (B) HPC-SL and (C) HPC-L.

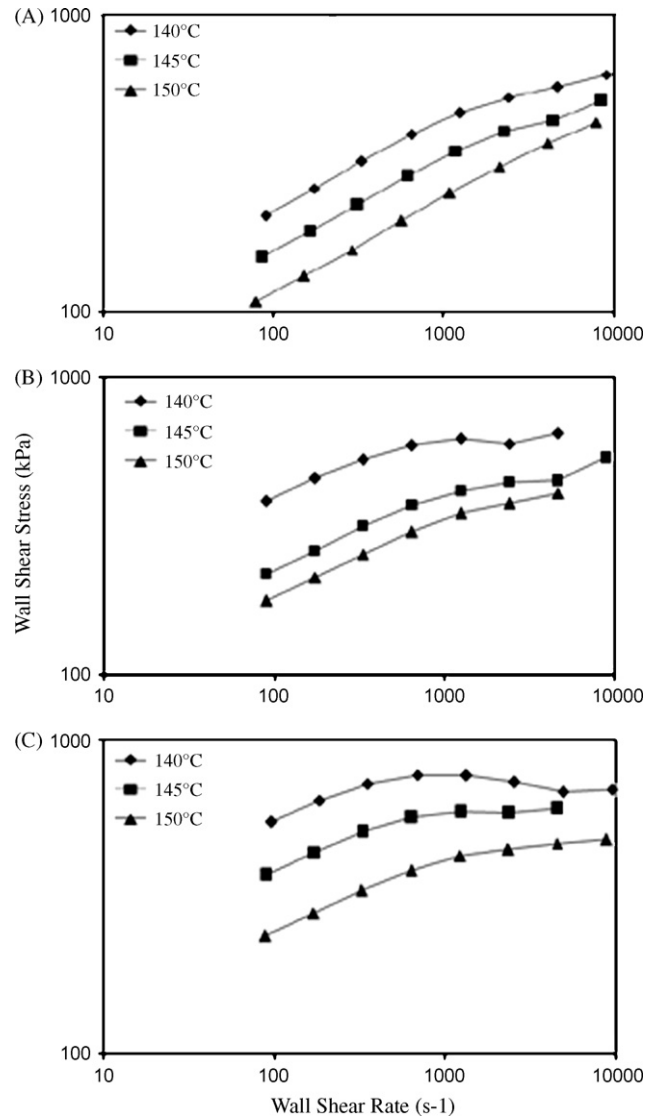


Fig. 4. Effect of shear rate on corrected shear stress at different temperatures (A) HPC-SSL; (B) HPC-SL and (C) HPC-L.

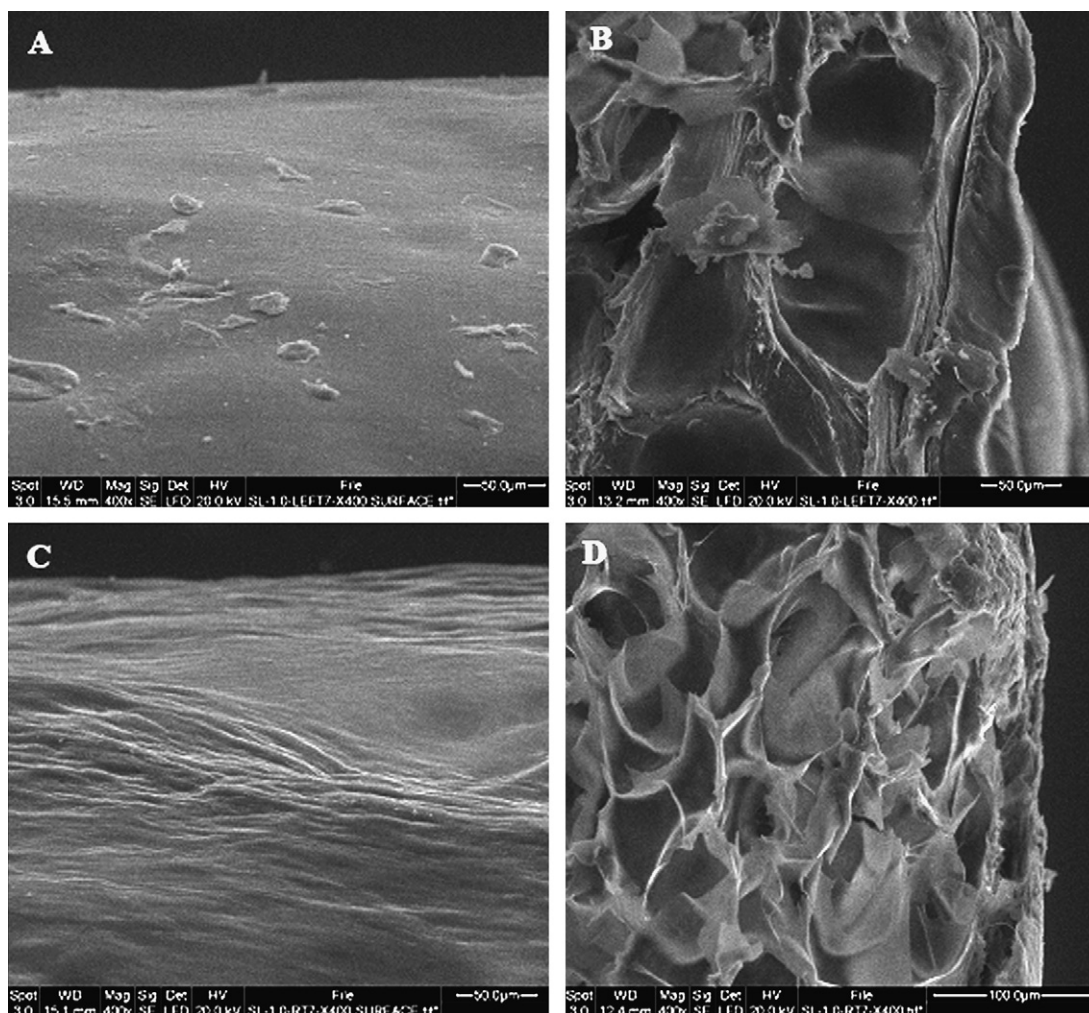


Fig. 5. Appearance of surface roughness and foaming in SL grade extrudate at a temperature of 140°C and wall shear rate of 2590 s^{-1} : (A) long die outer surface; (B) long die cross-section; (C) short die outer surface and (D) short die cross-section.

at shear rates above 1000 s^{-1} . This is typical for many polymer melts and occurs as a result of lower values of shear thinning index (i.e. higher degree of shear thinning) at lower temperatures. It can also be observed from Fig. 3 that viscosity above shear strain rates greater than 1000 s^{-1} deviated from the power law model. This can be seen more clearly from plots of wall shear stress against wall shear rate as shown in Fig. 4. Wall shear stress increased with rate in all cases with a gradually diminishing gradient due to the shear thinning nature of the melts. However, at rates significantly above 1000 s^{-1} step changes or discontinuities in the curves were observed in several cases. This indicates that the melt flow in this region may no longer follow the power law model so care should be taken when using it to make pressure drop or flow rate predictions in this region of shear strain rates. The observed step change in the shear stress versus shear strain rate appeared to become more pronounced with increasing molecular weight and decreasing temperature, i.e. with increasing viscosity. Deviation from the power law is likely to result from a breakdown of the assumptions on which the model is based, namely (i) zero fluid velocity at the wall, (ii) fluid streamlines are parallel to the wall, (iii) uniform hydrostatic pressure across any radial section of the capillary and (iv) flow is viscometric. The most likely causes of deviation from power law at high rates are melt flow instabilities and non-zero velocity at the die wall (i.e. wall slip). Surface roughness and in some cases foaming was observed for extrudate exiting the capillary dies at high shear rates

as shown in images obtained from scanning electron microscopic (SEM) images shown in Fig. 5, which suggests that flow instabilities and/or slip occurred. The onset of surface instabilities correlated with the discontinuities observed in Figs. 3 and 4, and therefore occurred at lower rates for higher molecular weight grades. Generation of instabilities during melt extrusion of polymers has been reported for many polymers used in the plastic industry [22,23] and have been observed to occur above a critical value of wall shear stress. Deviations from the power law model have been reported to correlate with flow instabilities [24] and from the zero wall velocity assumption [25]. The onset of foaming was found to be independent of rate by reversing the order of test stages shown in Table 1. Instabilities were formed at high strain rates as with tests carried out in the original order, but foaming occurred in the low rate stages at the end of the test, suggesting a dependence upon time and/or pressure rather than rate.

The relationship between K and average molecular weight is shown in Fig. 6. At each of the measured melt temperatures, K increased with increasing molecular weight. The rise appeared to be exponential in nature. Sensitivity of shear viscosity to set melt temperature was also found to increase with molecular weight, as shown in Fig. 7. This finding is in agreement with previous work [18] which concluded that the temperature and pressure sensitivity of a polymer melt was directly related to the size and complexity of the polymer molecule.

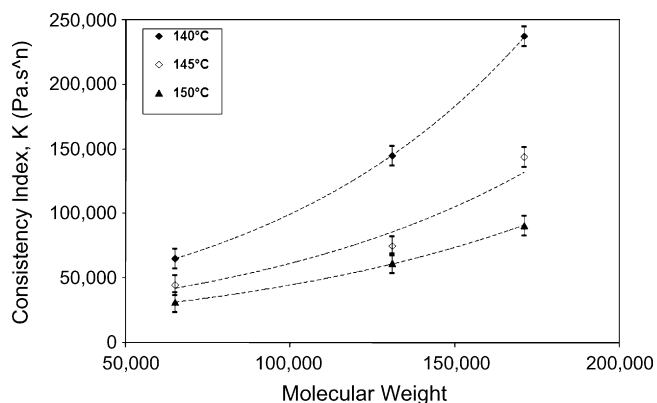


Fig. 6. Relationship between melt consistency index and weight average molecular weight at three set temperatures, with exponential fits (error bars show $\pm 1 \times$ standard deviation).

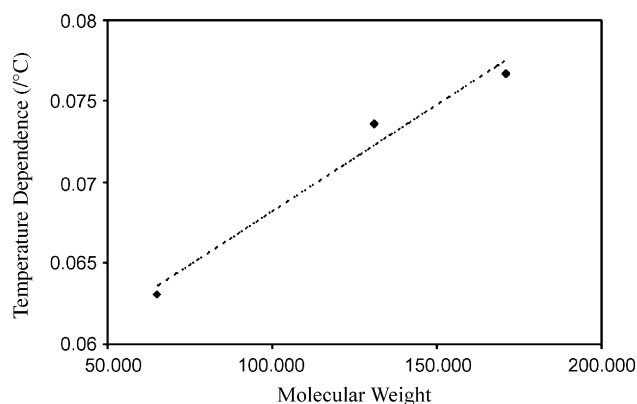


Fig. 7. Relationship between temperature sensitivity of shear viscosity and weight average molecular weight, with linear fit.

Orifice die entry pressure drops are plotted against processing rate for each of the three grades and temperatures studied (Fig. 8). Orifice die entrance pressure drop (P_0), sometimes termed 'entry pressure' is created due to sudden contraction of the fluid at the die entry region and is therefore a measure of the materials resistance to tensile or stretching flow. Two techniques are commonly used for the determination of P_0 . Bagley observed that a plot of pressure drop versus die length to diameter ratio (subsequently called a Bagley plot) gave a straight line with positive intercept [26]. This implied that through using several different length dies it is possible to extrapolate back to obtain a zero length pressure drop. Although this extrapolation can provide a reasonable prediction of

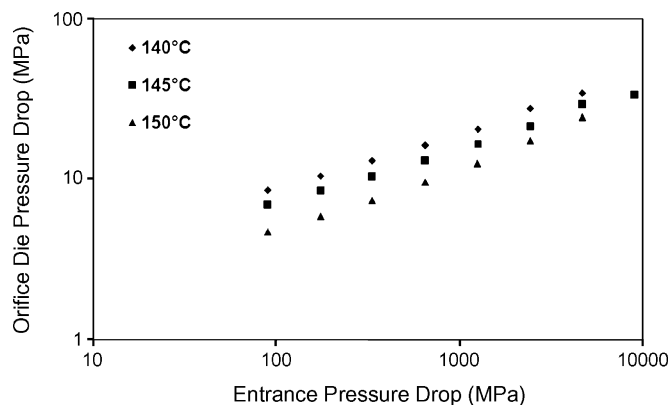


Fig. 8. Effect of shear rate on die entry pressure at different temperatures for HPC-SL.

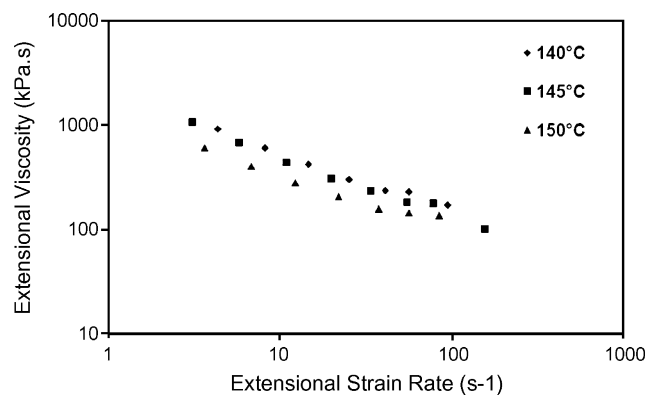


Fig. 9. Extensional viscosity vs. extensional strain rate at different temperatures for HPC-SL.

entry pressure drop, it does not take into account nonlinearities in the Bagley plot and is subject to errors in the extrapolation process. A more accurate method of P_0 determination is by direct measurement using an orifice die with effectively zero length [27]. The most common method is to use two dies, one long die ($L:D = 16:1$) and one orifice die ($L:D \approx 0$), carried out simultaneously in the case of twin bore rheometers. From Fig. 6, die entry pressure drop can be seen to increase with wall shear rate and molecular weight and decrease with increasing temperature.

Extensional viscosities and extensional strain rates were calculated using Eqs. (7) and (9), respectively and the relationship between these two parameters is shown in Fig. 9. Extensional viscosity was found to decrease with increase strain rate (i.e. tension thinning) at the rates examined, and increased with increasing molecular weight and decreasing melt temperature, in similar manner to that shown by shear viscosity. Extensional viscosities were observed to be a factor of between 260 and 2900 higher than shear viscosity, which is typical for polymer melts. Ratio of extensional to shear viscosity increased with increasing molecular weight and decreasing temperature, i.e. with increasing melt viscosity. The ratio between extensional viscosity and Newtonian shear viscosity is termed the Trouton ratio [28] and is 3:1 for Newtonian fluids. For non-Newtonian polymers at high strain rates, the ratio is several orders of magnitude greater, and provides an indication of the relative importance of extensional flow, which is highly dependent upon molecular structure.

An understanding of the relationships between shear and extensional flows with temperature, processing rate and molecular weight is a useful tool for process design, optimisation and troubleshooting. The characterisations carried out during these studies have shown that the flow behaviour of the HPC grades studied was typical of many thermoplastic polymers of relatively high molecular weight, up to a certain processing rate. Above this critical rate or stress significant instabilities were generated, in particular for the two higher molecular weight HPC-SL and HPC-L grades at low temperatures. Two distinct instabilities were observed; the appearance of a surface roughness at high shear rates which was followed by the formation of a foamed extrudate core. The prior has been reported by many workers for polymers such as polyethylene, polypropylene, polystyrene and polybutadiene but formation of foam without [25] addition of additive has not been reported. It is important to understand the basic cause of this phenomenon, which is potentially advantageous to drug delivery system design, and is therefore the subject of ongoing research in our laboratories.

4. Conclusions

Shear and extensional melt flow behaviour of hydroxypropyl cellulose was measured using capillary rheometry and the effects of

molecular weight, temperature and processing rate were quantified. All of the grades studied exhibited shear-thinning behaviour and a dependence upon melt temperature and molecular weight. The power law was found to be a suitable model for shear flow behaviour up to shear strain rates of approximately 1000 s^{-1} . Above this rate, measured shear viscosities deviated from the power law model and surface instabilities were observed in the extrudate, particularly for higher molecular weight grades. Foaming of the extrudate occurred in both capillary dies at high shear strain rates, and appeared to initiate inside the rheometer barrels prior to entry into the capillary dies. The mechanism of foaming is unclear at present and warrants further investigation. Extension viscosity of all grades studied was found to decrease with increasing temperature and increasing processing rate.

Acknowledgements

Anant Paradkar is thankful to British Council for UK-India Education and Research Initiative (UKERI) Fellowship, Bharati Vidyapeeth University, Pune for the sabbatical leave. Authors are thankful to Nippon Soda Ltd., Japan and Nisso Chemical Europe GmbH, Germany, for the gift samples of HPC and Malvern instruments, UK for technical support.

References

- [1] C. Leuner, J. Dressman, *Eur. J. Pharm. Biopharm.* 50 (2000) 47–60.
- [2] G. Verreck, K. Six, G. Van den Mooter, L. Baert, J. Peeters, M.E. Brewster, *Int. J. Pharm.* 251 (2003) 165–174.
- [3] J.E. Patterson, M.B. James, A.H. Forster, R.W. Lancaster, J.M. Butler, T. Rades, *Int. J. Pharm.* 336 (2007) 22–34.
- [4] M.A. Repka, J.W. McGinity, *J. Control. Rel.* 70 (2001) 341–351.
- [5] S. Prodduturi, K.L. Urman, J.U. Otaigbe, M.A. Repka, *AAPS PharmSciTech* 8 (50) (2007) E1–E10.
- [6] J. Breitenbach, *Eur. J. Pharm. Biopharm.* 54 (2002) 107–117.
- [7] C.R. Young, J.J. Koleng, J.W. McGinity, *Int. J. Pharm.* 242 (2002) 87–92.
- [8] M.M. Crowley, B. Schroeder, A. Fredersdorf, S. Obara, M. Talarico, S. Kucera, J.W. McGinity, *Int. J. Pharm.* 269 (2004) 509–522.
- [9] M. Fukuda, N.A. Peppas, J.W. McGinity, *J. Control. Rel.* 115 (2006) 121–129.
- [10] G. Verreck, A. Decorte, K. Heymans, J. Adriaensen, D. Liu, D. Tomasko, A. Arien, J. Peeters, G. Van den Mooter, M.E. Brewster, *Int. J. Pharm.* 327 (2006) 45–50.
- [11] J.G. Lyons, M. Hallinan, J.E. Kennedy, D.M. Devine, L.M. Geever, P. Blackie, C.L. Higginbotham, *Int. J. Pharm.* 329 (2007) 62–71.
- [12] R.J. Chokshi, H.K. Sandhu, R.M. Iyer, N.H. Shah, A.W. Malick, H. Zia, *J. Pharm. Sci.* 94 (2005) 2463–2474.
- [13] L.G. Lyons, P. Blackie, C.L. Higginbotham, *Int. J. Pharm.* 35 (2008) 201–208.
- [14] C. Rauwedaal, *Polymer Extrusion*, 2nd ed., Hanser Publishing, Munich, 1990.
- [15] F.N. Cogswell, *Trans. Soc. Rheol.* 16 (1972) 383–403.
- [16] D.M. Binding, J. Now-Newton, *Fluid Mech.* 27 (1988) 173–189.
- [17] M.L. Sentmanat, *Rheol. Acta* 43 (2004) 657–669.
- [18] T. Sedlacek, M. Zatloukal, P. Filip, A. Boldizar, P. Saha, *Polym. Eng. Sci.* 44 (2004) 1328–1337.
- [19] F.N. Cogswell, *Polymer Melt Rheology: A Guide for Industrial Practice*, Godwin, London, 1981.
- [20] R.A. Mendelson, *Polym. Eng. Sci.* 8 (1968) 235–240.
- [21] L. Williams, R.F. Landel, J.D. Ferry, *J. Am. Chem. Soc.* 77 (1955) 3701–3707.
- [22] S.G. Hatzikiriakos, K.B. Migler, *Polymer Processing Instabilities; Control and Understanding*, Marcel Dekker, New York, 2005.
- [23] J.F. Agassant, D.R. Arda, C. Comeaud, A. Merten, H. Mundstedt, M.R. Mackley, L. Rober, B. Vergnes, *Int. Polym. Proc.* 11 (2006) 239–255.
- [24] J.P. Tordella, *J. App. Phys.* 27 (1956) 454–458.
- [25] S.G. Hatzikiriakos, J.M. Dealy, *J. Rheol.* 36 (1992) 845–884.
- [26] E.B. Bagley, *J. App. Phys.* 28 (1957) 624–627.
- [27] J.M. Dealy, *Melt Rheology and its Role in Plastics Processing*, Kluwer Academic Publishers, Amsterdam, 1999.
- [28] F.T. Trouton, *Proc. R. Soc. A* 77 (1906) 426–440.